Journal of Materials Chemistry C



PAPER

View Article Online



Cite this: DOI: 10.1039/d0tc01257b

Photoinduced cationic polycondensation in solid state towards ultralow band gap conjugated polymers†

Xunshan Liu, D Valerii Sharapov, Zhen Zhang, Forwood Wiser, Mohammad Ahmad Awais and Luping Yu*

A photoinduced cationic polycondensation towards the synthesis of a thieno[3,4-b]thiophene (TT) based homopolymer PTT-L was described. The reaction mechanism was investigated by employing a series of control experiments. It was found that the polymerization initiated with a light-induced radical formation, followed by a cationic propagation, all in solid state, at room temperature, and without any catalyst or solvent. In addition, a reference polymer (PTT-Ni) was synthesized *via* Kumada catalyst transfer polycondensation (KCTP) to assist in structural characterization of polymer PTT-L. It was shown that both polymers exhibit analogous optical, thermal, electrochemical and electrical properties. This polymerization process can be utilized as a mean to form patterned PTT-L films.

Received 10th March 2020, Accepted 20th April 2020

DOI: 10.1039/d0tc01257b

rsc.li/materials-c

1. Introduction

This manuscript reports an accidental discovery of a photo-induced solid state polymerization of monobromo-thieno[3,4-*b*]-thiophene (M1) to form NIR conjugated polymers with an ultralow optical band gap. Our results have important implications in both synthesis of conjugated polymers and the mechanism for cationic chain-growth polymerizations involving aromatic monomers.

Since nineteen eighties, cationic polymerizations have been extensively studied towards applications in both industry and academia. As in all chain-growth polymerizations, initiation remains the essential step in cationic polymerizations. Towards this end, a myriad of inexpensive, and environmentally benign initiating systems have been developed. Among these systems, photoinitiation has shown promise as it is inexpensive, green and non-invasive. Photoinitiation can be further categorized into direct initiation and multicomponent initiation. Monomers suitable for cationic polymerizations are vinylic and cyclic compounds containing electron-donating (epoxides, vinyl ethers, alkenes, cyclic ethers, and lactones) groups that can stabilize the newly formed cationic species. However, aromatic monomers rarely undergo cationic polymerizations towards fully conjugated polymers. Therefore, the development of

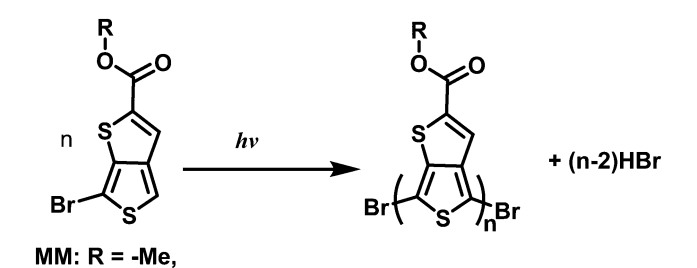
cationic polymerizations for aromatic systems is interesting for the synthesis of advanced materials.

Conjugated polymeric materials have been actively investigated towards applications in electrical as well as optical devices. For example, those with narrow bandgaps have found applications in organic solar cells, NIR photodetectors, and biological sensing and imaging. Moreover, most of these polymers are synthesized *via* transition metal catalyzed coupling reactions, such as Kumada catalyst transfer polycondensation (KCTP) and Suzuki catalyst transfer polymerization (SCTP). Recently, we discovered that a polythienothiophene (PTT) polymer can be synthesized *via* photoinduced polymerization in solid state (Scheme 1). Detailed studies lead us to propose a unique mechanism: photoinduced cationic polycondensation. PTT has previously been reported to exhibit interesting properties due to its extremely low energy band gap and a broad absorption in Vis-NIR spectral range. This photoinduced polycondensation

Department of Chemistry and The James Franck Institute, The University of Chicago, 929 East 57th Street, Chicago, IL 60637, USA.

E-mail: lupingyu@uchicago.edu

† Electronic supplementary information (ESI) available. See DOI: 10.1039/d0tc01257b



PTT-L: R= -ethylhexyl

Scheme 1 The photoinduced solid state polymerization.

M1: R= -ethylhexyl

reaction is novel, and shall have broader applications in synthesis of other polymers since the scope of monomer's structure can be extended. This paper presents detailed studies on the synthesis of the polymer and the mechanism of polymerization. Physical properties associated with these polymers are also discussed.

2. Results and discussion

While we were attempting to synthesize compounds based on TT, we prepared the compound M1 as an intermediate (Scheme 1), which was found to be extremely light sensitive. When exposed to light without adding any external reagents, it easily reacted in solid state to form a blue solid. When the alkyl group of the monomer is a methyl (MM), the resulting blue solid is insoluble. However, when an ethylhexyl group was used, the resulting solid is soluble in organic solvents, such as chloroform and chlorobenzene. Gel permeation chromatography studies indicated that these solids were polymeric materials (PTT-L) with molecular weights around 4.5 kg mol⁻¹ and a narrow polydispersity (Table 1). It was also observed that hydrogen bromide gas was a byproduct of the reaction, which was confirmed by a reaction with trivinyl compound (see ESI†).

To identify the polymer structure, we synthesized a PTT homopolymer **PTT-Ni** via KCTP reaction (Scheme 2).^{17,18} GPC, NMR and MALDI mass spectroscopic studies confirmed that these two polymers exhibit similar spectroscopic features (see ESI†). UV-Vis spectroscopic studies indicated that both polymers exhibit a strong absorption in NIR region with a maximum around 1000 nm and an optical bandgap of 0.73 eV. Thus, we can conclude that the resulting polymers have similar structures.

There have been several reports on homo-polymerization of aromatic dihalide monomers via different mechanisms. In addition, thermally activated solid state coupling of dihalothiophenes is well documented.¹⁹ Non-halothiophenes are also

Table 1 Polymerization results and thermal properties of the two polymers

Polymers	Yields (%)	$M_{\rm n}$	$M_{\rm w}^{\ a} \left({\rm kg \ mol}^{-1} \right)$	PDI	$T_{\rm d}^{\ b}$ (°C)
PTT-Ni	83	3.68	4.45	1.21	300
PTT-L	92	4.48	5.23	1.17	303

^a Determined by GPC in CHCl₃ based on polystyrene standards. ^b Decomposition temperature, determined by TGA in nitrogen, based on 5% weight loss.

Scheme 2 Synthesis of PTT-Ni via KCTP reaction

known to undergo photoinduced stepwise polymerization via photolysis.²⁰ Moreover, thiophene monomers can undergo oxidative polymerization (either electrochemically or chemically) to form polymers.²¹ With monomer M1, however, none of the above mechanisms can explain the observations of the following control experiments.

We proposed two possible mechanisms: photoinduced radical polymerization and photoinduced cationic polymerization. After systematically carrying out a series of control experiments, and carefully investigating the structures and properties of the resulting polymers, we concluded that it is most likely a photoinduced cationic polycondensation. This is an interesting example of a photoinduced cationic polymerization of aromatic monomers towards the synthesis of conjugated polymers.

2.1 Control experiments

Initially, we proposed a radical reaction mechanism to explain the formation of polymers in the solid state (Scheme 3). It is well known that the C-Br bond in bromothiophene can be photolytically cleaved to form thiophenyl and bromo radicals. 22,23 We hypothesized that the thiophenyl radical will add to the monomer M1, followed by the elimination of HBr. It is also likely that the thiophenyl radicals can dimerize to form a dimer, which can then react with another radical. Repeating these steps leads to the formation of a polymer chain.

The four control experiments (entries 1, 2, 3 and 4 in Table 2) seem to support the first photolytic cleavage step. Experiments 1 and 2 showed that the polymerization would not occur when the monomers are stored in the dark, while experiments 3 and 4 showed that the polymerization occurs both in N2 and O2 under light. Entry 10 showed that the solid state reaction of monomer M1 containing 1 equivalent of 1,4-benzoquinone (a well know radical inhibitor²⁴) did not occur and the monomer is recovered. Since quinone is also an effective quencher for the excited state, the photolytical cleavage of C-Br bond did not occur in this mixture.

However, two control experiments (entries 5, and 6) provided contrary evidence. In these experiments, one equivalent of 1-hexanethiol was mixed with monomer M1 (20 mg of M1 was transferred to a vial with a stirrer under dark, the vial was fully wrapped with aluminum foil, sealed with a cap, protected with N2. One equivalent of 1-hexanethiol was transferred to the vial through syringe with stirring. The prepared vials were then exposed to light (entry 5) or kept in dark (entry 6)). While the mixture in the dark (entry 6) was stable, it polymerized under light (entry 5) although much slow in comparison to entry 3. While the polymerization in entry 3 completed within ten minutes, the initiation of the polymerization in entry 5 took 4 hours and completed overnight. The results indicated that the polymerization could not be a radical reaction since thiol compounds are known efficient agents for chain transfer in free radical reactions.²⁵ In this reaction, one equivalent of thiol compound was used under which condition a radical polymerization cannot proceed. The slow polymerization can be related to the slow formation of small amount of bromine molecules. Experiment entry 7 (14 hours) and entry 9 (14 hours) gave further

Scheme 3 Proposed radical polymerization.

Table 2 Monomers and related results of the control experiments

Polymers

		Reaction conditions			Polymerization results ^a			
Entry	Monomers	Light	Gas	Reagents	Time	$M_{\rm w}$ (kg mol ⁻¹)	PDI	Yield (%)
1	M1	No	O_2	_	14 h	_	_	
2	M1	No	N_2	_	14 h	_	_	
3	M1	Yes	N_2		10 min	5.23	1.17	95
4	M1	Yes	O_2		10 min	3.37	1.04	94
5	M1	Yes	N_2	1-Hexanethiol	14 h	3.74	1.03	95
6	M1	No	N_2	1-Hexanethiol	14 h	_	_	
7	M1	No	N_2	AIBN (80 °C)	14 h	3.26	1.10	92
8	M1	No	N_2	AIBN (60 °C)	14 h	3.52	1.08	93
9	M1	Yes	N_2	Ethyl acrylate	14 h	3.16	1.05	90
10	M1	Yes	N_2	1,4-Benzoquinone	14 h	_	_	
11	M1	Yes	N_2	Et ₃ N	14 h	_	_	
12	M1	No	O_2	HBr	14 h	_	_	
13	M1	No	O_2	Br_2	10 min	3.30	1.02	93
14	M1	Yes	O_2	$CHCl_3$	3 days	3.68	1.10	94
15	M2	Yes	O_2	DCM	10 min	3.31	1.03	96
16	9	Yes	O_2	DCM	14 h	_	_	
17	9	No	O_2	Br_2	10 min	3.33	1.04	95
18	9	No	O_2	Br ₂ /DCM	10 min	2.93	1.10	93
19	M1	Yes	N_2	TEMPO	14 h			
20	M1	Yes	N_2	$TEMPO/Br_2$	14 h	Oligomer		
21	M3	No	O_2	-	14 h	_	_	
22	M3	No	N_2	$\mathrm{Br_2/DCM}$	14 h	_	_	

 $[^]a$ All the newly formed polymers are characterized with GPC against polystyrene standard. $M_{\rm w}$ is weight-average molecular weight. Other than stated, all the control experiments were carried out at room temperature.

evidences to support that the reaction is not radical polymerization. In entry 7, a mixture prepared from monomer M1 containing radical initiator, azobisisobutyronitrile (AIBN, 5% weight) was heated at 80 °C. In entry 9, ethyl acrylate of 10 equivalents was

mixed with monomer M1. It was found that monomer M1 polymerized under both conditions. MALDI-TOF studies showed that the end groups of polymer chains were the same as the polymers obtained in other conditions. We did not observe any

alkyl groups from AIBN and the incorporation of ethyl acrylate species in the formed polymers. Entry 8 indicated that the polymerization can also proceed with heating at the temperature (60 °C) that AIBN is stable. Based on these results, we can conclude that the radical mechanism is not responsible for the polymerization as shown in Scheme 3.

The experiment in entry 11 indicated that triethylamine (1 equivalent) inhibited polymerization. This implies two things: firstly, triethylamine is a known quencher for certain photoexcited states which can inhibit C-Br bond cleavage or can act as radical chain transfer agent. Secondly, the HBr formed is important for polymerization. Experiment in entry 12 showed that the monomer did not undergo polymerization by simply adding HBr (initiator scale about 5%). However, polymerization did occur (entry 13) when a small amount (initiator scale about 5%) of bromine was added to the monomer. Therefore, the bromine formed during the photolytic process is likely the origin for the polymerization. Further studies (entry 14) in the reaction conditions showed that the polymerization also occurred under light in the solution state by dissolving the monomer M1 in CHCl₃ (10 mg mL⁻¹) although the reaction was much slower than that in the solid state. While in solid state (entry 4) the reaction completed within ten minutes, the transparent solution started turning to yellow after 5 hours, and it took 3 days when the color changed to blue, indicating the formation of polymers.

Furthermore, the monomer M2 (Scheme 4) was synthesized and used in the experiment (entry 15) which is similarly reactive towards photoinduced polymerization.

Three more experiments (entries 16-18) offer further support to the hypothesis that bromine is the crucial source for polymerization. The compound 9 (Scheme 4) was used as a monomer for these experiments. When it was exposed to light without adding any other reagents, it was stable. When Br₂ was added, the polymerization proceeded in both solid and the solution state. In experiment entry 19, two equivalents of TEMPO (2,2,6,6-tetramethyl-1-piperidinyloxy) were mixed with the monomer and exposed to light under N2. The color of mixture did not change, MALDI-TOF experiments indicated that polymerization did not occur. Further addition of a small amounts (about 5%) of Br₂ (entry 20) to this mixture, oligomers was formed, further indicating the Br₂ as an initiator.

The mechanistic function of bromine could possibly be the charge transfer from electron rich monomer to form radical

cations, which can then dimerize to form a dication. The dication will then be converted into neutral dibromo-dithienothiophene (M3). However, this mechanism is in contradiction with the observation that dibromo-dithienothiophene is stable both photochemically and toward bromine as shown in the experiments (entries 21 and 22). This is also true for dibromothienothiophene (M). It seems that in these two compounds, the C-Br bonds are photochemically more stable than that in monomer M1.

A crucial observation is that only a short time exposure to visible light was all that was required to complete the reaction. A monomer sample that briefly exposed to light (about 1 min) and was wrapped with aluminum foil and stored in the refrigerator was found polymerized the next day. This observation further supports that radical reaction is not the working mechanism since radical reaction normally require higher temperature to provide activation energy than that for cationic polymerization.

An important question for the cationic polymerization is which position in monomer 1 is attacked by the reactive cation. Combining the results from experiments 15, 18, and 22, leads us to conclude that only C-H position is the reactive site that can be attacked by the cation while the C-Br side is unreactive. The DFT calculation results for the monomer M1 support this statement (Fig. S16 and Table S1, ESI†). The geometry optimization and energy calculations of M1 were conducted at B3LYP level of theory using 6-31G** basis set. Optimized geometry was used to calculate Mulliken charge distribution in the molecule. Our results showed that carbon of a C-Br bond carries a Mulliken charge of -0.252 a.u. while the carbon of a C-H bond discussed above carries a charge of -0.368 a.u. A more negative partial charge on this atom will facilitate preferential attack by the cation, which is reflected in our proposed mechanism.

Based on all the control experiments and DFT calculations, we propose the mechanism shown in Scheme 5. First, C-Br bonds of the monomers were cleaved photolytically by absorbing light, followed by a radical combination to form a dimer and bromine molecules. The bromine electrophilically attack the monomer M1 to form a living cation, a typical textbook process for bromination in electron rich compounds. The initiated cation exists within its resonance structure, which can be stabilized by the lone pair electrons in its neighboring bromine and sulfur atoms. The newly formed cation attacks another monomer and passes the positive charge to the next TT unit. This structure becomes non-conjugated and has a strong

Scheme 4 Structures of different monomers.

Scheme 5 A photoinduced cationic polycondensation mechanism.

driving force to eliminate an HBr molecule to further form a cation with a quinoidal structure. This process can then repeat itself until the polymerization is stopped when the terminal proton is extracted by a bromo anion. The quinoidal structure then converts into a conjugated PTT.

2.2 Terminal group analysis

MALDI-TOF spectrometry was used to determine the molecular weight of the polymers and to further analyze the terminal groups. According to the proposed mechanism, our polymers appear to be terminated with two bromine atoms. However, the mass spectra did not show the existence of bromine atoms. These results were then further confirmed by elemental analysis of the resulting polymers (see ESI†), which did not show any Br content.

Fig. 1 shows the mass spectrum of PTT-L. Here, the molecular weight difference between each peak is about 294 Daltons, which is the molecular weight of a TT unit. For instance, the peak at 1225 means a polymer with 4 TT units, which are

terminated with an -OH and -O₂H groups. Similarly, the peak at 1519 Daltons stand for 5 TT units while the one at 1813 Daltons stand for 6 TT units, and so on. To make it clearer, a zoomed spectrum of the peak at 1813 Daltons is shown in Fig. 2. Here, we see 4 groups of peaks with multiple isotope peaks within each group. The difference between each group amounts to 16 Daltons, corresponding to a different number of O atoms at the termini of the polymers. The small peaks around the assigned highest peaks in Fig. 2 are isotope peak of each. All the peaks shown in Fig. 1 exhibit the same trend as the peak at 1813 Daltons. This analysis proves the mechanism discussed above as we assume that the C-Br bond at the polymer chain termini are possibly cleaved when exposed to light and a polymer radical(s) is formed. The dimer M3 is stable due to strong interaction between two bromo groups. The C-Br bonds in the dibromo-terminated polymers are similar to those in monobromo-thienothiopenens (Br-TT), which tend to be cleaved and form radicals. Unlike small molecules, the newly formed radicals are too massive to recombine with each other. Thus, they tend to react with O₂ in the air

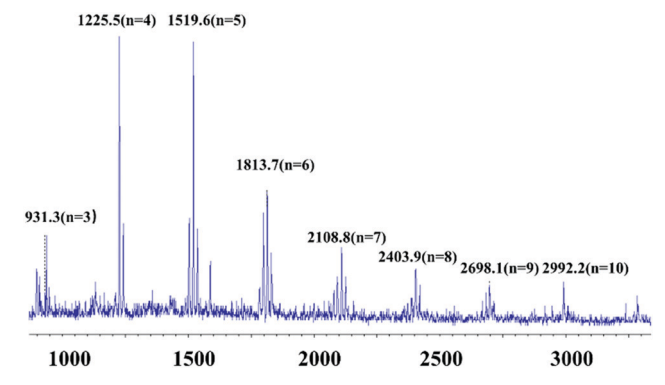


Fig. 1 Maldi-Tof mass spectrum of PTT-L.

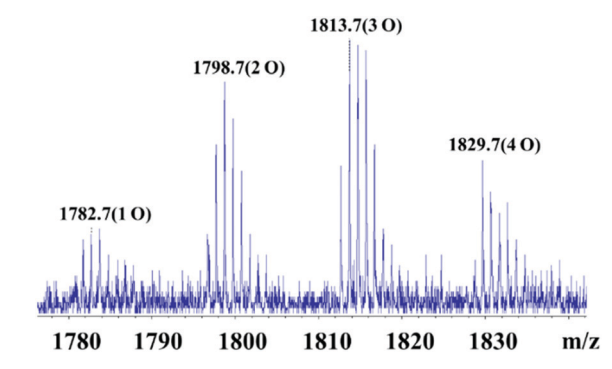


Fig. 2 A zoomed spectrum around the peak 1813.7.

2.3 Optical properties

The photophysical properties of the two polymers (PTT-Ni and PTT-L) were investigated using UV-Vis-NIR spectroscopy. The key physical properties are summarized in Table 3. Both two polymers show a very broad absorption (500 nm to 1700 nm) in visible-NIR region (Fig. 3). PTT-Ni and PTT-L exhibit their absorption maxima at 1017 nm and 910 nm, respectively. This difference may be due to the differences in regioregularity between the polymers. While polymer PTT-Ni is a regio-random polymer as the two bromine atoms of monomer M have no specificity for Kumada coupling reaction, PTT-L is supposed to be a head-tail regionegular polymer. Absorption spectra for thin films are broadened as compared to the spectra in solution (Fig. 4). Interestingly, the absorption peak for PTT-Ni is blue-shifted, while the absorption peak for PTT-L is red-shifted when compared to their corresponding solution spectra. This is probably caused by the difference in the aggregation state, because the two polymers should have different conformation based on the mechanisms we proposed. Moreover, the optical band gaps (E_{o}^{opt}) of thin films were found to be 0.73 eV, and 0.76 eV for PTT-Ni, and PTT-L, respectively.

2.4 Electrochemical and electrical properties

Electrochemical spectra of both polymers were investigated by cyclic voltammetry (CV). The CV curves and its corresponding data (Fig. 5 and Table 3) indicated that these polymers are electroactive. The redox potentials were first referenced to the ferrocene/ferrocenium redox couple (Fc/Fc⁺) which is 0.35 V vs. SCE. The redox potential of Fc/Fc $^+$ was assumed to be at -4.8 eV to relative to the vacuum.²⁶ Then HOMO/LUMO energy levels and electrochemical energy gaps (E_g^{ec}) of our copolymers were calculated as per the following equations:

HOMO =
$$-(E_{ox} + 4.45)$$
 (eV);
LUMO = $-(E_{red} + 4.45)$ (eV);
 $E_{g}^{ec} = (E_{ox} - E_{red})$ (eV)

The onset oxidation potentials (E_{ox}) were found to be 0.55 and 0.65 V for PTT-Ni and PTT-L, corresponding to the HOMO energy levels of -5.00 eV and -5.10 eV, respectively. The LUMO

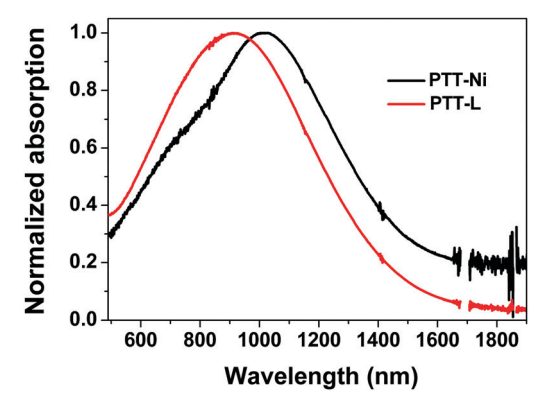


Fig. 3 Vis-NIR absorption spectra of the polymers in CHCl₃.

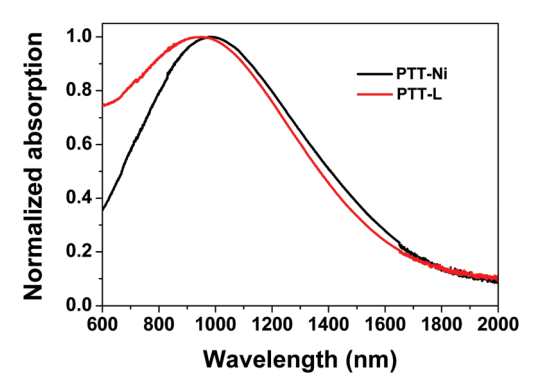


Fig. 4 Vis-NIR absorption spectra of the polymer films

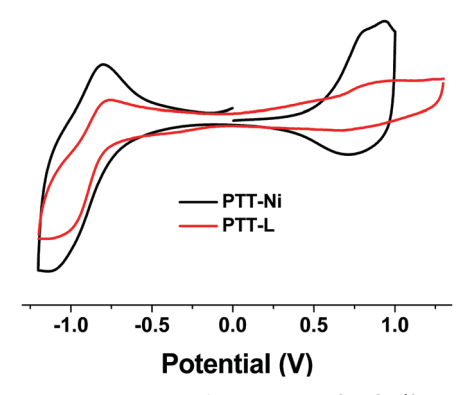


Fig. 5 Cyclic voltammograms of polymers in CH₃CN/0.1 M Bu₄NPF₆ at 100 mV s⁻¹.

energy levels of PTT-Ni and PTT-L were calculated to be -3.75and -3.67 eV, indicating a low band gap of 1.25 eV and 1.43 eV,

Table 3 Optical and electrochemical properties of the two polymers

	Solution $\lambda_{s,max}^{a}$ (nm)	Film $\lambda_{f,max}$ (nm)	Film λ_{edge} (nm)				
Polymers	Abs.	Abs.	Abs.	$E_{\mathbf{g}}^{\mathbf{opt}\;b}\left(\mathbf{eV}\right)$	HOMO (eV)	LUMO (eV)	Egec (eV)
PTT-Ni	1017	982	1692	0.73	-5.00	-3.75	1.25
PTT-L	910	948	1632	0.76	-5.10	3.67	1.43

^a Measured in chloroform solution. ^b Band gap estimated from the optical absorption band edge of the films.

respectively. These low band gaps are in good agreement with their broad absorption in the visible-NIR region.

2.5 Electrical properties

To investigate the electrical properties of both polymers, we measured space-charge limited carrier (SCLC) mobilities of hole-only and electron-only devices (Fig. S18, ESI†). Hole-only devices were fabricated in a configuration ITO/PEDOT:PSS/ active layer/MoO₃/Ag and electron-only devices were ITO/ZnO/ active layer/Ca/Al. ITO glasses were ultrasonicated in chloroform, acetone and propanol-2 for 15 min each and then cleaned in UV/ozone cleaner for 30 min. For hole-only devices PEDOT:PSS water suspension purchased from HERAEUS was spin coated at 6000 rpm/60 seconds and then annealed under vacuum at 100 °C for 30 min. For electron-only devices ZnO precursor solution of Zn(CH₃COO)₂, 2-aminoethanol and 2-methoxyethanol was spin coated at 4000 rpm/40 seconds and annealed in air at 200 °C for 30 minutes. The active layer was spin coated from chloroform/chlorobenzene solution at 1000 rpm/60 seconds and annealed in nitrogen glove box at 120 °C for 30 minutes. Top electrodes 8 nm MoO₃/90 nm Ag and 20 nm Ca/80 nm Al were thermally deposited under vacuum $(10^{-7}-10^{-6} \text{ Torr})$ through a shadow mask. *I–V* curves of the devices were measured and SCLC region of the curves

was fitted with the Gurney–Mott equation: $J = \frac{9 \epsilon \epsilon_0 \mu (V - V_{\rm bi})^2}{2 \epsilon_0 V_{\rm bi}}$ where J – current density, ε – dielectric constant (assumed 3), ε_0 = dielectric permittivity of vacuum, μ – mobility, V – applied voltage, V_{bi} - built-in voltage, L - thickness of the film (measured with AFM). It was found that PTT-Ni exhibits hole and electron mobilities of $(1.2 \pm 0.4) \times 10^{-4} \text{ cm}^2 \text{ V}^{-1} \text{ s}^{-1}$ and $(4.2 \pm 1.6) \times 10^{-5} \text{ cm}^2 \text{ V}^{-1} \text{ s}^{-1}$, with the hole mobility/electron mobility ratio 2.86. PTT-L, however, was found to exhibit higher mobilities of (2.7 \pm 1.7) \times 10⁻⁴ cm² V⁻¹ s⁻¹ for holes and $(9.3 \pm 1.5) \times 10^{-5} \text{ cm}^2 \text{ V}^{-1} \text{ s}^{-1}$ for electrons, with the hole mobility/electron mobility ratio 2.90. The higher hole and electron mobilities in PTT-L maybe due to its higher regioregularity according to the polymerization mechanism we proposed, also lack of Ni catalyst residual in PTT-L will also help to enhance the mobilities. The higher the regioregularity of polymers, the higher will be charge carrier mobilities.^{27,28}

2.6 Morphology investigation

In order to investigate the morphology and packing of **PTT-L** and **PTT-Ni** polymers we measured GIWAXS scattering profiles of its polymer films (Fig. S19, ESI†). General scattering profiles of both the polymers are very similar, demonstrating lamellar scattering peak at around 0.29 Å⁻¹ and π - π stacking peaks in the 1.4–1.7 Å⁻¹ region. Both the polymers here are quite amorphous and lack preferential orientation. Lamellar peak at 0.29 Å⁻¹ is present in out-of-plane and in-plane directions for both the polymers. The same is true of the π - π stacking peaks. It should be noted that second order scattering (200) peak at 0.53 Å⁻¹ is observed in **PTT-L**'s profile. This indicates that **PTT-L** has a more ordered structure than **PTT-Ni** which is



Fig. 6 A pattern of M1 (left) and the laser cut black mask (right).

consistent with PTT-L being more regio-regular, according to our proposed mechanism.

2.7 Patterning

Since the compound M1 is sensitive to light and can be photochemically polymerized, we use it as a patterning material. A PMMA solution (30 mg mL⁻¹ in ethyl acetate) was spin coated on a glass slide, and then annealed at 150 °C to modify the substrate. Then a solution of M1 (40 mg mL⁻¹ in hexanes) was spin-coated on the modified slide. At this stage, the slide was still transparent. A laser cut mask (Fig. 6) was put on the top of the M1 coated slide. The slide was then exposed to visible light for 12 h. It was observed that the color of exposed part slowly changed light yellow, yellow, light green and deep green. The mask was removed after 12 hours, and the slide was washed several times with methanol. Then the pattern was formed as showed in Fig. 6. The pattern obtained showed relatively high resolution. More detailed studies are needed to further improve patterning quality by completely removing the dull shadows by using straight light source in a dark environment and carefully prepare the monomer films. The obtained preliminary results have demonstrated a valuable potential to use this solid state polymerization to form NIR polymers patterning materials.

3. Conclusions

A bromothieno[3,4-b]thiophene monomer (M1) was polymerized *via* photoinduced solid state polycondensation to form a NIR conjugated polymer with an ultralow optical band gap. Control experiments support the polymerization involves two steps: photocleavage of C–Br bond and bromine initiated cationic polymerization. The obtained polymers have been investigated and applied as patterning materials. The nature of this reaction provides opportunities to further extend the scope of this polymerization. This reaction exhibits certain advantages that can be exploited for further applications such as in patterning and in the development of advanced materials.

Conflicts of interest

There are no conflicts to declare.

Acknowledgements

This work was supported by NSF (Chem-1802274), partially supported by the University of Chicago Materials Research Science and Engineering Center, which is funded by the National Science Foundation under award number DMR-1420709. We also acknowledge partial support by Samsung GRO project. This work made use of the shared facilities at the University of Chicago Materials Research Science and Engineering Center, supported by National Science Foundation under award number DMR-1420709. This research used resources of the Advanced Photon Source, a U.S. Department of Energy (DOE) Office of Science User Facility operated for the DOE Office of Science by Argonne National Laboratory under Contract No. DE-AC02-06CH11357.

References

- 1 M. Miyamoto, M. Sawamoto and T. Higashimura, Macromolecules, 1984, 17, 265.
- 2 R. Faust and J. P. Kennedy, J. Polym. Sci., Part A: Polym. Chem., 1987, 25, 1847-1869.
- 3 O. Michaudel, V. Kottisch and B. P. Fors, Angew. Chem., Int. Ed., 2017, 56, 9670.
- 4 J. V. Crivello and J. H. W. Lam, Macromolecules, 1977,
- 5 V. Kottisch, Q. Michaudel and B. P. Fors, J. Am. Chem. Soc., 2016, 138, 15535.
- 6 C. Fu, J. Xu and C. Boyer, Chem. Commun., 2016, 52, 7126.
- 7 K. A. Ogawa, A. E. Goetz and A. J. Boydston, J. Am. Chem. Soc., 2015, 137, 1400-1403.
- 8 B. Bonillo and T. M. Swager, J. Am. Chem. Soc., 2012, **134**, 18916.
- 9 L. Dou, Y. Liu, Z. Hong, G. Li and Y. Yang, Chem. Rev., 2015, **115**, 12633.
- 10 Y. Braeken, S. Cheruku, A. Ethirajan and W. Maes, Materials, 2017, 10, 1420.

- 11 H. Sun, S. Zhang, Y. Yang, X. Li, H. Zhan and Y. Cheng, Macromol. Chem. Phys., 2016, 217, 2726.
- 12 K. Lee and G. A. Sotzing, Macromolecules, 2001, 34, 5746.
- 13 G. A. Sotzing and K. Lee, Macromolecules, 2002, 35, 7281.
- 14 M. A. Invernale, V. Seshadri, D. M. D. Mamangun, Y. Ding, J. Filloramo and G. A. Sotzing, Chem. Mater., 2009, 21, 3332.
- 15 J. H. Park, Y. G. Seo, D. H. Yoon, Y.-S. Lee, S.-H. Lee, M. Pyo and K. Zong, Eur. Polym. J., 2010, 46, 1790.
- 16 F. Liu, G. L. Espejo, S. Qiu, M. M. Oliva, J. Pina, J. S. Seixas de Melo, J. Casado and X. Zhu, J. Am. Chem. Soc., 2015, 137, 10357.
- 17 A. Yokoyama, R. Miyakoshi and T. Yokozawa, Macromolecules, 2004. 37, 1169.
- 18 R. Miyakoshi, A. Yokoyama and T. Yokozawa, J. Am. Chem. Soc., 2005, 127, 17542.
- 19 H. Meng, D. F. Perepichka, M. Bendikov, F. Wudl, G. Z. Pan, W. Yu, W. Dong and S. Brown, J. Am. Chem. Soc., 2003, 125, 15151.
- 20 Y. Yagci, S. Jockusch and N. J. Turro, Macromolecules, 2007,
- 21 R. D. McCullough, Adv. Mater., 1998, 10, 93.
- 22 F. Zhang, Z. Cao, X. Qin, Y. Liu, Y. Wang and B. Zhang, Acta Phys.-Chim. Sin., 2008, 24, 1335.
- 23 F. Elisei, L. Latterini, G. G. Aloisi and M. D'Auria, J. Phys. Chem., 1995, 99, 5365.
- 24 A. Debuigne, J.-R. Caille and R. Jérôme, Macromolecules, 2005, 38, 6310.
- 25 C. Henríquez, C. Bueno, E. A. Lissi and M. Encinas, *Polymer*, 2003, 44, 59.
- 26 Y. Li, Y. Cao, J. Gao, D. Wang, G. Yu and A. J. Heeger, Synth. Met., 1999, 99, 243.
- 27 J.-S. Kim, J.-H. Kim, W. Lee, H. Yu, H. J. Kim, I. Song, M. Shin, J. H. Oh, U. Jeong, T.-S. Kim and B. J. Kim, Macromolecules, 2015, 48, 4339.
- 28 R. Mauer, M. Kastler and F. Laquai, Adv. Funct. Mater., 2010, 20, 2085.